# FT-IR Study of Bridging Carbonyl Structure of $H_2FeRu_3(CO)_{13}$ Trapped in Noble Gas Matrices and Adsorbed on Oxide Surfaces

S. DOBOS, A. BECK

*Institute of Isotopes, Hungarian Academy of Sciences, H-1525 Budapest, P.O.B. 77, Hungary*

S. NUNZIANTE-CESARO and M. BARBESCHI

*Centro Studi Termodin. Chim. Alte Temp., University of Rome, P. 1e A. Moro, Rome, Italy*

(Received November 12, 1986)

## Abstract

Infrared spectra ranging from 4000 to 180 $cm^{-1}$ of $H_2FeRu_3(CO)_{13}$ isolated in argon and nitrogen matrices were recorded. Minimum two conformations of $H_2FeRu_3(CO)_{13}$ and two fragments ($Ru_3(CO)_{12}$ and $Fe(CO)_5$) have been individuated. By quantitative treatment of the spectral range of bridging carbonyl stretching modes performing on spectra of $H_2FeRu_3(CO)_{13}$ matrix-isolated and adsorbed on $SiO_2$ and $Al_2O_3$ supports, two main double bridging structures of different geometries have been identified and angles between bridging carbonyls have been estimated. Additional double and single bridging carbonyls, characteristic of the individual supported cluster systems, have also been detected.

## Introduction

Recently, using infrared spectroscopy combined with quantitative treatment of the spectra, we have studied the bridging CO structure of the nonrigid molecules of $Fe_3(CO)_{13}$, $Fe_2Ru(CO)_{12}$ and $H_2FeRu_3(CO)_{13}$, in different solvents and in the crystal form [1, 2]. The above cluster molecules are of the highest importance as precursors in preparing bimetallic catalysts supported on metal oxides like silica and alumina. The interaction of clusters with an oxide support is assumed to be responsible for the final activity of the catalyst. Several papers have dealt with the terminal stretching region of the infrared spectra [3–7]. We believe that the study of the structure of bridging carbonyls will supply valuable information about the behaviour of the molecules physisorbed or chemisorbed on the oxide surfaces. The molecule of $H_2FeRu_3(CO)_{13}$ contains two bridging groups. From infrared intensity data we are able to estimate the angle of the C–O bonds in this double bridging system. As we have shown this angle is very sensitive to the surroundings of the molecule, for instance to the polarity of a solvent [1, 2]. However, due to the very low intensity of spectral bands belonging to bridging carbonyls, it is rather difficult to use this region of the spectra of adsorbed molecules for quantitative treatment. The molecule of $H_2FeRu_3(CO)_{13}$ is less rigid in comparison with that of $Fe_3(CO)_{12}$ or $Fe_2Ru(CO)_{12}$ and a higher part of the molecule is in the bridged form, so the intensity of bridging CO bands is somewhat higher [2]. This is why we have chosen it for the present study. In order to assign the spectra to possible structures we will take into consideration the structures identified in our previous paper [2]. Furthermore, we have recorded the spectra of $H_2FeRu_3(CO)_{13}$ in a pseudo-gaseous state *i.e.* in low temperature argon and nitrogen matrices, by a method that is often a useful tool in detecting whether the co-existence of different conformers of a molecule might be expected, or to modellize structures of adsorbed species.

## Experimental

The method given in ref. 8 was used to produce $H_2FeRu_3(CO)_{13}$.

### *Matrix Isolation Experiments*

The experimental apparatus consisted of a Bruker Interferometer IFS 113 v, under vacuum, and an Air Product and Chemicals closed-cycle refrigeration system (DISPLEX CSA 202). The cold finger, holding a CsI window, was free to rotate in the vacuum shroud, where the pressure was kept at $10^{-7}$ torr. The window temperature was monitored through a Chromel-gold (0.07% Fe) thermocouple to a precision of 0.5 K.

The sample was used without further purification. It was evaporated from a home-made pyrex cell heated by a standardized Kanthal resistancy. Deposition temperature ranged from 309 to 329 K.

Nitrogen and argon of high purity (Caracciolo Oss. 99.9%) were employed as isolating gases: the flow rate was controlled by a standardized needle valve.

0020-1693/87/$3.50

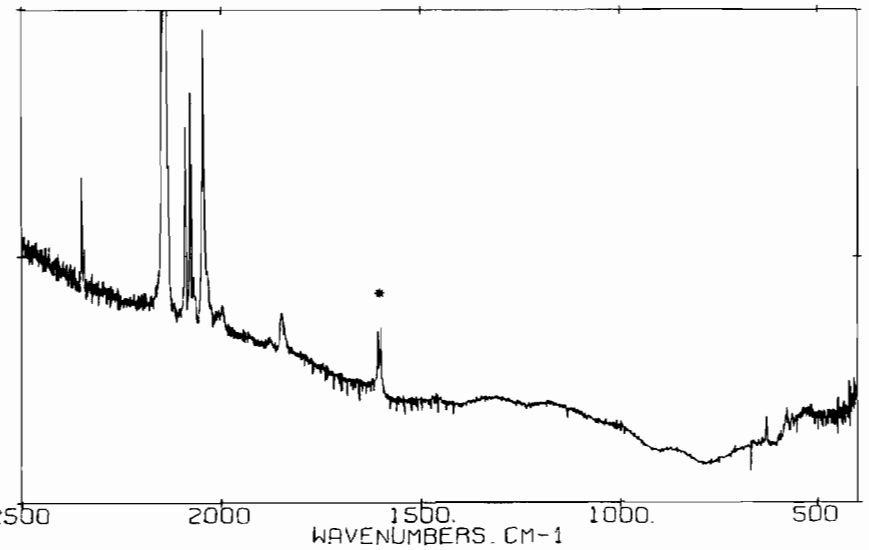


Fig. 1. Infrared spectrum of $H_2FeRu_3(CO)_{13}$ isolated in argon matrix.

The average value was around 1 mmol/h and deposition time lasted from 20 to 60 min. More intense spectra were obtained by prolonging the deposition time at a given temperature.

Good isolation degree was empirically checked by increasing the matrix gas flow keeping the evaporation temperature. In addition, annealing cycles were performed for most experiments.

The usual spectral range was 4000–400 $cm^{-1}$, but in the case of intense ($N_2$ matrix, low temperature sample evaporation) spectra the range was extended upto the transparency limit of the CsI at 180 $cm^{-1}$. The accuracy was 0.5 $cm^{-1}$ in the whole spectral range.

*Adsorption Experiments*

Alumina and silica were obtained from Degussa ($Al_2O_3$ C) and Cabot Corporation (Cab-O-Sil HS5), respectively, and heated *in vacuo* at 573 K for 12 h (by this treatment the alumina and silica still remain hydrated: hydroxile monolayer coverage about 60% [6–7]), then contacted with the pentane solution of the cluster compound. The supported cluster was dried under vacuum. Calculated metal loadings were about 1%.

In the experiments performed in Nujol, immediately after the evaporation of the solvent, the sample was wetted by paraffin oil (Nujol) and put between two KBr windows and from time to time the infrared spectrum was recorded.

In the temperature decomposition experiments the supported cluster was dried in vacuum for 12 h and pressed into wafers (10 $mg/cm^2$), which were then placed in a heatable vacuum IR cell. Infrared spectra, under vacuum or $H_2$ stream, were recorded at temperatures ranging from 303 to 413 K.

Finally the spectrum of $H_2FeRu_3(CO)_{13}$ in KBr pellet was also recorded.

For all reported spectra a 200-scan data accumulation was carried out at a resolution of 4 $cm^{-1}$, using a Digilab FTS-20C interferometer equipped with a Data General Nova 3 computer. Silica or alumina wafers were used as references.

To analyse the spectra in the region of CO stretching modes of bridging carbonyls, the sum of maximum 8 Gaussians was fitted to the data points of the baseline corrected spectra. The angles $\phi$ between the C–O bonds of adjacent bridging carbonyls were calculated using the integrated intensities of the asymmetric and symmetric CO stretching modes [1]. However, angles $\phi$ calculated for adsorbed molecules are values of lower accuracy in comparison to those calculated from spectra recorded in solutions of $H_2FeRu_3(CO)_{13}$.

## Results and Discussion

*Pseudo-gaseous State*

The survey spectrum of $H_2FeRu_3(CO)_{13}$ isolated in argon is reported in Fig. 1. All observed bands recorded in both argon and nitrogen matrices are summarized in Table I with their assignment.

Nitrogen and argon isolated spectra are substantially identical: however, in the former case a number of modes is splitted into sharp components whose relative intensities depend on the sample evaporation temperature. As an example, in Fig. 2 the behaviour of the CO terminal stretches at about 2045 and 1995 $cm^{-1}$ and the bridging CO mode at 1846 $cm^{-1}$, at two different temperatures, is shown.

TABLE 1. Infrared Spectra of $H_2FeRu_3(CO)_{13}$ in Low Temperature Matrices and in Solution

| Nitrogen | Argon | n-Hexane | Assignment |
|---|---|---|---|
| 2144vs | 2144vs | | CO |
| 2116.3w | 2115.1w | | |
| 2112.9w | 2112.9vw | 2111w | terminal CO stretching |
| 2092m | 2092.4w, sh | | |
| 2089.5s | 2088.7s | | |
| 2084.7w, sh | 2084w, sh | 2084s | terminal CO stretching |
| 2077.7s | 2077s | | |
| 2076.3s | 2076s | | |
| 2072.7w, sh | 2072.2vw, sh | 2073s | terminal CO stretching |
| 2067w | 2066.6w | | $Ru_3(CO)_{12}$ |
| 2046.8vs | 2050.9w,sh | | |
| 2045vs | | | |
| 2044.3vs | 2043.7vs | 2042vs | terminal CO stretching |
| | 2038.4w, sh | | |
| 2037.3m | | | |
| 2035.5mw | 2035.7w, br | | |
| 2034.3w | 2034w | | $Ru_3(CO)_{12}$ |
| 2031.4w | 2032.6w | 2032w | terminal CO stretching |
| 2025.5w | 2026vw | | $Fe(CO)_5$ |
| 2023.2mw | 2023vw | 2022sh | terminal CO stretching |
| 2014w | | | |
| 2012.8w | | | $Ru_3(CO)_{12}$ |
| 2011.4w | 2010vw | 2012sh | terminal CO stretching |
| 2005w | | | $Fe(CO)_5$ |
| 2003.8w | 2003.6w | | |
| 1996.7m | 1997mw | | |
| 1995.2m | 1994.5mw | 1992m | terminal CO stretching |
| 1994mw | | | |
| 1990w, sh | | | |
| | | 1973vw | terminal CO stretching |
| | | 1962vw | |
| 1931vvw | | 1932vw | terminal CO stretching |
| 1878.8w, sh | 1876.9w | 1882w | bridging CO stretching |
| 1874.7mw | | | |
| 1850.8vw, sh | | | |
| 1846m | 1847.5mw | 1854m | bridging CO stretching |
| 1844w, sh | | | |
| 1817vw, b | | | |
| 638.9m | 639m | | M–C stretching |
| 630.7sh | | | |
| 628.8m | 627.5w | | M–C stretching |
| 577.2m | 576.7w | | M–C stretching |
| 562.2mw | 562.5vw | | M–C stretching |
| 535w | 536mw | | M–CO deformation |
| 435mw | 435w | | M–CO deformation |
| 238vw | | | Fe–Ru stretching |

Multiple trapping sites cannot be invoked as an explanation because annealing cycles did not produce any change. The presence of impurities like water affecting the guest molecule can also be excluded on grounds of experimental evidence. Three more hypothesis can be formulated to explain multiplicity: (i) decomposition of $H_2FeRu_3(CO)_{13}$; (ii) presence of aggregates; (iii) presence of conformers.

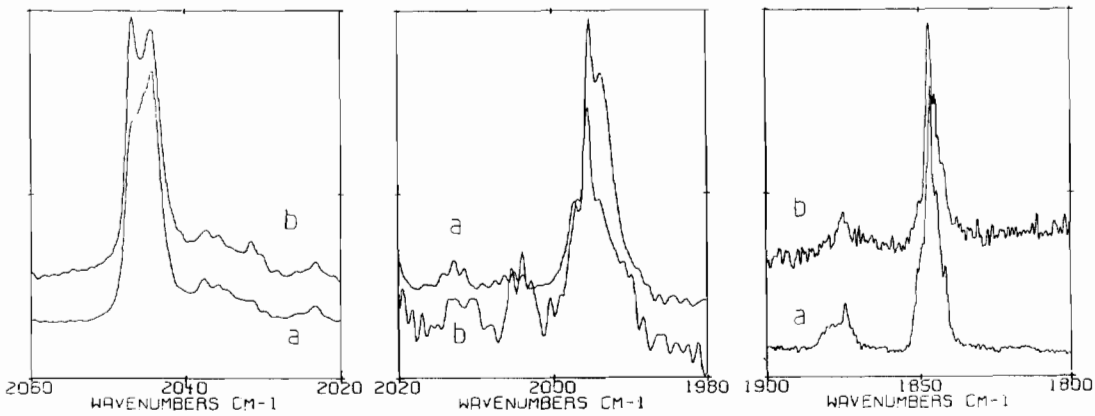


Fig. 2. Expanded infrared spectra of $H_2FeRu_3(CO)_{13}$ isolated in nitrogen. Sample evaporation temperature: (a) 309 K, (b) 329 K.

With regard to the first point, the sharp band observed at 2144 $cm^{-1}$, both in nitrogen and in argon, suggests a partial decomposition of the molecule. Two fragments have been spectroscopically individuated: $Ru_3(CO)_{12}$ characterized by its strongest absorptions at 2067, 2034.3 and 2012.8 $cm^{-1}$ [9] and $Fe(CO)_5$ by its frequencies at 2025.7 and 2005 $cm^{-1}$ [10]. It is worth noting that intensities of the above bands increase with the deposition temperature, still remaining very weak in our spectra, suggesting a quite negligible effect. On the other hand, the appearance of these fragments supports the conclusion of ref. 7 that the first step of the interaction of $H_2FeRu_3(CO)_{13}$ with the alumina surface is decomposition into $Ru_3(CO)_{12}$ and $Fe(CO)_5$.

However a mechanism can be hypothesized that a single molecule gives rise to one of the two possible fragments upon the closer proximity of the CO groups to the iron or to the three ruthenium atoms. In both cases only unstable metal carbonyls are likely to be formed contributing to the free CO absorption, with a metal residue.

Point (ii) can be easily ruled out, first because of the annealing evidence and the isolation degree previously discussed. In addition, the band components affected by the temperature are very sharp and lie at the higher frequency side of the multiplets, which is not the usual behavior for aggregates.

In conclusion, the third explanation, *i.e.* the presence of conformers, seems to be the most reasonable. As pointed out by NMR $^{13}C$ measurements, $H_2FeRu_3(CO)_{13}$ undergoes at room temperature dynamic processes involving both ligand and metal core mobility [11, 12]. It is therefore reasonable to assume that the matrix patterns freeze a number of the possible conformations of the molecule during its flight from the furnace to the cold finger. It is also plausible that the population of more energetic states is higher with the increase of the temperature.

*Adsorbed/Chemisorbed States*

$H_2FeRu_3(CO)_{13}$, like $Fe_2Ru(CO)_{12}$. adsorbed from solutions on hydrated alumina surfaces, rapidly decomposes into monometallic dicarbonyl species $Ru^0(CO)_2$, $Ru^{II}(CO)_2$ and $Ru^{III}(CO)_2$ and iron is oxidized to $Fe^{2+}$ and $Fe^{3+}$ during a standard drying process in vacuum [6]. Even immediately after impregnation, metal–metal bonds split and no bridging carbonyls can be detected. As we have shown, the surface reaction can be slown down by the competitive adsorption of large hydrocarbon molecules, e.g. by wetting the sample with paraffin oil (Nujol) [7].

For the sake of comparison, in Fig. 3a–d we collected some characteristic survey spectra of the systems in question in both the terminal and bridging carbonyl stretching region. A detailed study of the terminal stretching of the $H_2FeRu_3(CO)_{13}$ molecule together with other FeRu bimetallic clusters adsorbed on the silica support will be presented elsewhere [13].

In Fig. 4a–n the spectra of bridging carbonyls together with their Gaussian components are shown, while numerical results of the analysis of the spectra are collected in Table II.

*$H_2FeRu_3(CO)_{13}/Al_2O_3$/Nujol*

In Fig. 4a is shown the spectral range of the stretching modes of bridging carbonyls of the system $H_2FeRu_3(CO)_{13}/Al_2O_3$/Nujol recorded immediately after impregnation ($t = 0$). Under the experimental spectrum the Gaussian components are also recorded. In the first row of Table II the numerical data, like frequencies and integrated intensities of the Gaussian components, are shown. In the last two rows we have completed Table II with the analogous data for n-hexane and dichloromethane solutions taken from ref. 2. Taking into account these results, we can divide the components into pairs, which represent the symmetric and asymmetric combinations of CO

TABLE II. Infrared Frequencies $\nu_{A-I}$ ($cm^{-1}$) and Integrated Intensities $I_{A-I}$ (arbitrary units) of the Gaussian Components of the Bridging Carbonyl Bands and Calculated Angles $\phi_{AB-EF}$ (grades) Between the C–O Bonds in Double Bridging Structures

| System | $R_{T/Br}$ | $\nu_{A(A')}$<br>$\nu_{B(B')}$ | $I_{A(A')}$<br>$I_{B(B')}$ | $\phi_{AB}$<br>$\phi_{A'B'}$ | $\nu_{C(C')}$<br>$\nu_{D(D')}$ | $I_{C(C')}$<br>$I_{D(D')}$ | $\phi_{CD}$<br>$\phi_{C'D'}$ | $\nu_E$<br>$\nu_F$ | $I_E$<br>$I_F$ | $\phi_{EF}$ | $\nu_S$ | $I_S$ | $\nu_H$ | $I_H$ | $\nu_I$ | $I_I$ | $\Sigma I$ |
|---|---|---|---|---|---|---|---|---|---|---|---|---|---|---|---|---|---|
| $Al_2O_3$/Nujol | | 1882.3 | 31 | | 1877 | 12 | | 1896 | 20 | | | | | | | | |
| | 20.7 | | | 109 | | | 81 | | | 68 | 1908 | 13 | | | | | 155 |
| $t = 0$ | | 1853.3 | 61 | | 1839 | 8.8 | | 1864 | 9 | | | | | | | | |
| $Al_2O_3$/Nujol | | 1881.9 | 14 | | 1874 | 4.5 | | 1895.5 | 26 | | | | | | | | |
| | 26.5 | | | 109 | | | 67 | | | 52 | 1910.5 | 6 | | | | | 87 |
| $t$ = 40 min | | 1853 | 28 | | 1839 | 2 | | 1863.8 | 6.3 | | | | | | | | |
| $SiO_2$/Nujol | | 1883 | 18 | | 1872.8 | 31 | | 1890 | 23 | | | | | | | | |
| | 7.1 | | | 137 | | | 118 | | | | | | 1820 | 57 | 1804 | 72 | 409 |
| $t = 0$ | | 1854.6 | 122 | | 1839.7 | 86 | | | | | | | | | | | |
| $SiO_2$/Nujol | | 1882.1 | 12 | | 1871.7 | 15 | | | | | | | | | | | |
| | 7.8 | | | 137 | | | 123 | | | | | | 1822 | 54 | 1803 | 81 | 238 |
| $t$ = 1 h | | 1852.8 | 79 | | 1840 | 51 | | | | | | | | | | | |
| $SiO_2$/Nujol | | 1882.1 | 11 | | 1871.2 | 16 | | | | | | | | | | | |
| | 7.6 | | | 139 | | | 121 | | | | | | 1822.5 | 44 | 1805 | 98 | 254 |
| $t$ = 3 h | | 1852.6 | 78 | | 1839.2 | 51 | | | | | | | | | | | |
| $SiO_2$/wafer/vacuum | | 1886 | 79 | | 1867 | 650 | | | | | | | | | | | |
| | 5.6 | | | 104 | | | 56 | | | | | | 1816 | 1083 | 1776 | 30 | 2152 |
| $T$ = 293 K | | 1847 | 128 | | 1831 | 182 | | | | | | | | | | | |
| $SiO_2$/wafer/vacuum | | 1886 | 79 | | 1866.5 | 650 | | | | | | | | | | | |
| | 5.7 | | | 106 | | | 56 | | | | | | 1816 | 1038 | 1773 | 30 | 2088 |
| $T$ = 373 K | | 1846 | 139 | | 1831 | 182 | | | | | | | | | | | |
| $SiO_2$/wafer/vacuum | | 1887 | 83 | | 1865.2 | 439 | | | | | | | | | | | |
| | 7.3 | | | 103 | | | 64 | | | | | | 1816 | 667 | 1773 | 30 | 1491 |
| $T$ = 373 K | | 1846 | 133 | | 1830 | 169 | | | | | | | | | | | |
| $SiO_2$/wafer/vacuum | | 1886.5 | 83 | | 1866 | 194 | | | | | | | | | | | |
| | 13.2 | | | 104 | | | 67 | | | | | | 1816 | 172 | 1794 | 35 | 670 |
| $T$ = 393 K | | 1845.8 | 135 | | 1830 | 86 | | | | | | | | | | | |
| $SiO_2$/wafer/vacuum | | 1888.5 | 48 | | 1868.5 | 135 | | | | | | | | | | | |
| | 15.8 | | | 120 | | | 64 | | | | | | 1817 | 52 | 1798 | 33 | 463 |
| $T$ = 413 K | | 1846.6 | 142 | | 1830 | 53 | | | | | | | | | | | |

*(continued)*

TABLE II. *(continued)*

| System | $R_{T/Br}$ | $\nu_{A(A')}$ $\nu_{B(B')}$ | $I_{A(A')}$ $I_{B(B')}$ | $\phi_{AB}$ $\phi_{A'B'}$ | $\nu_{C(C')}$ $\nu_{D(D')}$ | $I_{C(C')}$ $I_{D(D')}$ | $\phi_{CD}$ $\phi_{C'D'}$ | $\nu_E$ $\nu_F$ | $I_E$ $I_F$ | $\phi_{EF}$ | $\nu_S$ | $I_S$ | $\nu_H$ | $I_H$ | $\nu_I$ | $I_I$ | $\Sigma I$ |
|---|---|---|---|---|---|---|---|---|---|---|---|---|---|---|---|---|---|
| $SiO_2$/wafer/$H_2$ | | 1886 | 65 | | 1875 | 105 | | | | | | | | | | | |
| | 8.6 | | | 111 | | | 60 | | | | | | 1821 | 1159 | | | 1502 |
| $T$ = 313 K | | 1860 | 138 | | 1844 | 35 | | | | | | | | | | | |
| $SiO_2$/wafer/$H_2$ | | 1886 | 65 | | 1874.5 | 98 | | | | | | | | | | | |
| | 8.9 | | | 108 | | | 64 | | | | | | 1821 | 1153 | | | 1476 |
| $T$ = 333 K | | 1860 | 121 | | 1843 | 39 | | | | | | | | | | | |
| $SiO_2$/wafer/$H_2$ | | 1855.2 | 70 | | 1869 | 124 | | | | | | | | | | | |
| | 13.4 | | | 127 | | | 60 | | | | | | 1818 | 639 | | | 1160 |
| $T$ = 353 K | | 1848 | 286 | | 1830 | 41 | | | | | | | | | | | |
| In KBr | | 1882 | 8 | | 1872 | 429 | | | | | | | | | | | |
| | 7.8 | | | 157 | | | 126 | | | | | | 1810 | 200 | | | 2464 |
| | | 1851.5 | 198 | | 1838 | 1629 | | | | | | | | | | | |
| In nitrogen matrix | | | | | 1874.6 | | | | | | | | | | | | |
| | 8.0 | | | | | | 141 | | | | | | | | | | |
| (high temp.)[a] | | | | | 1846 | | | | | | | | | | | | |
| In nitrogen matrix | | 1878.8 | 164 | | 1874.6 | 156 | | | | | | | | | | | |
| | 10.7 | | | 125 | | | 139 | | | | | | 1817 | 40 | | | 2076 |
| (low temp.)[b] | | 1850.8 | 618 | | 1846 | 1098 | | | | | | | | | | | |
| In argon matrix | | 1882 | | | | | | | | | | | | | | | |
| | 6.9 | | | 128 | | | | | | | | | | | | | |
| | | 1854 | | | | | | | | | | | | | | | |
| In $C_6H_{12}$ solution[c] | | 1882 | | | | | | | | | | | | | | | |
| | 7.9 | | | 141.6 | | | | | | | | | | | | | |
| | | 1854 | | | | | | | | | | | | | | | |
| In $CH_2Cl_2$ solution[c] | | | | | 1873 | | | | | | | | | | | | |
| | 10.2 | | | | | | 123.5 | | | | | | | | | | |
| | | | | | 1838 | | | | | | | | | | | | |

[a]Sample evaporation temperature 329 K. [b]Sample evaporation temperature 309 K. [c]Recalculated from intensity data given in ref. 2.

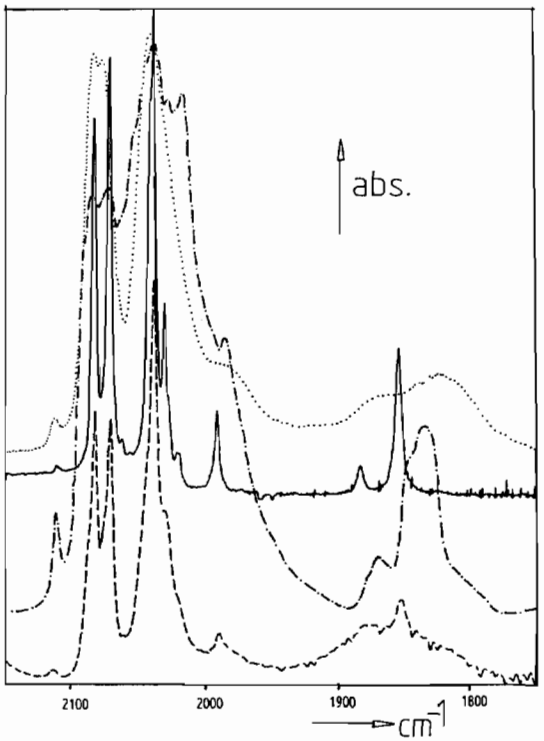


Fig. 3. Infrared spectra in terminal and bridging CO stretching region of $H_2FeRu_3(CO)_{13}$, recorded (a) ——, in n-hexane solution; (b) —·—, in KBr pellet; (c) — — —, adsorbed on system $Al_2O_3$/Nujol ($t$ = 0 min); and (d) ·····, adsorbed on system $SiO_2$/wafer/vacuum ($T$ = 303 K).

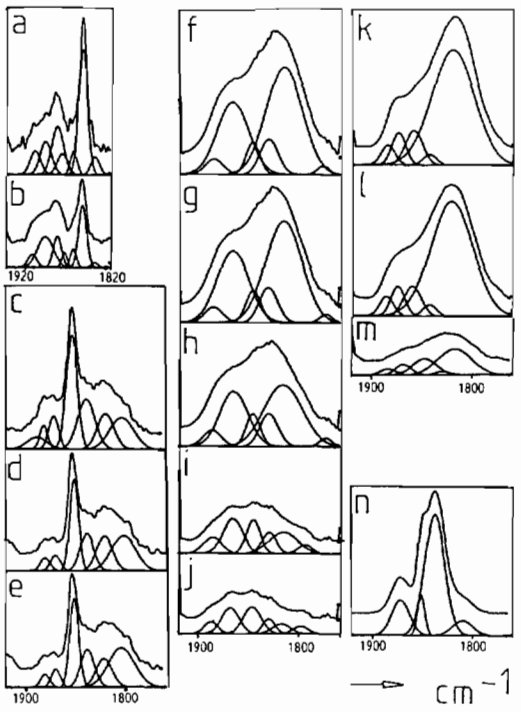


Fig. 4. Infrared spectra of bridging carbonyls and calculated Gaussian components for the systems: (a) $H_2FeRu_3(CO)_{13}$/$Al_2O_3$/Nujol, at $t$ = 0 min; (b) as a, but at $t$ = 40 min; (c) $H_2FeRu_3(CO)_{13}/SiO_2$/Nujol, at $t$ = 0 hour; (d) as c, but at $t$ = 1 h; (e) as c, but at $t$ = 3 h; (f) $H_2FeRu_3(CO)_{13}/SiO_2$/wafer/vacuum at $T$ = 303 K; (g) as f, but at $T$ = 333 K; (h) as f, but at $T$ = 373 K; (i) as f, but at $T$ = 393 K; (j) as f, but at $T$ = 413 K; (k) $H_2FeRu_3(CO)_{13}/SiO_2$/wafer/$H_2$ at $T$ = 313 K; (l) as k, but at $T$ = 333 K; (m) as k, but at $T$ = 353 K; (n) $H_2FeRu_3(CO)_{13}$ in KBr.

stretching modes of a double bridging carbonyl system. The frequencies of the first pair of bands $\nu_A$, $\nu_B$ (1882.3 and 1853 $cm^{-1}$) lie very close to those of the molecule in non-polar solvents, suggesting rather short C–O distances, with the only difference that the angle $\phi$ for this surface species is smaller. The frequencies of the second pair $\nu_C$, $\nu_D$ (1877 and 1839 $cm^{-1}$) correspond to those found in polar solvents (longer C–O distances); the respective angle $\phi$, however, is very small.

In the band system in question, a third pair of bands is also detectable ($\nu_E$, $\nu_F$) that has no analogue in other systems. This pair may represent bridging carbonyls with a very low angle $\phi$ and very short C–O distances, or bridging carbonyls bonded to oxidised metal atoms. The very small value of angle $\phi$ indicates highly distorted molecules.

A further band ($\nu_G$) appears at 1908 $cm^{-1}$, which should belong to very asymmetric or 'incipient' bridging carbonyls.

After 40 min the spectrum essentially contains the same components, however, the total amount of bridging carbonyls rapidly decreases; the intensity of pair $\nu_C$, $\nu_D$ ($I_C + I_D$) more rapidly than that of pair $\nu_A$, $\nu_B$, while the intensity of the pair $\nu_E$, $\nu_F$ slightly increases.

In the first column of Table II, $R_{T/Br}$ is the ratio between the total integrated intensity of the terminal carbonyl stretching region (2150–1920 $cm^{-1}$) and that of the bridging one (1920–1750 $cm^{-1}$). The value of $R_{T/Br}$ in solvents is about 7.9–10.2. In the system $Al_2O_3$/Nujol, $R_{T/Br}$ is significantly higher (20.7–26.5), showing that, at the very beginning of the interaction, the molecules on the surface already start decomposing (into $Ru_3(CO)_{12}$ and $Fe(CO)_5$ as shown in ref. 7) producing species without bridging carbonyls.

*$H_2FeRu_3(CO)_{13}/SiO_2$/Nujol*

The experimental spectra with the Gaussian components are seen in Fig. 4c–e. At the beginning of the interaction with the $SiO_2$ surface, the $H_2FeRu_3(CO)_{13}$ molecules are only sligthly distorted. The angle $\phi_{AB}$ (137°) is practically the same as in the solution of the non-polar n-hexane, while $\phi_{CD}$ (118–123°) corresponds to that in the polar dichloromethane. The contributions of both main species to the total intensity of the band system is practically

equal. The intensity ratio of the terminal and bridging carbonyl ($R_{T/Br}$ = 7.1–7.8) is also close to those in solutions.

Two additional spectral features ($\nu_H$ and $\nu_I$) appear at about 1822 and 1804 $cm^{-1}$, which can be assigned to supposedly monocarbonylic bridges with very long C–O distances, however, these bands are of very low intensity.

*$H_2FeRu_3(CO)_{13}/SiO_2$/wafer/vacuum*

In this type of experiment, after impregnation, the supported cluster was dried for 12 h in vacuum and then pressed into a wafer without wetting it with paraffin oil, then put in the infrared vacuum cell, in order to study the behaviour of bridging carbonyls during thermal treatment.

The experimental spectrum and the Gaussians are shown in Fig. 4f–i. Numerical data are given in Table II.

The spectrum contains, as main features, the pairs of bands $\nu_{A'}$, $\nu_{B'}$; $\nu_{C'}$, $\nu_{D'}$ and a broad band $\nu_H$ of great integrated intensity. The contribution of the main features to the overall intensity of the band system can be expressed by the ratios $(I_{A'} + I_{B'})$: $(I_{C'} + I_{D'})$:$(I_H)$ = 1:4:5, at 303 K. With increasing temperature $I_H$ rapidly decreases, $I_C + I_D$ decrease somewhat slower, while $I_A + I_B$ practically does not change. At $T$ = 413 K the ratios between intensities are $(I_{A'} + I_{B'})$:$(I_{C'} + I_{D'})$:$I_H$ = 1:1:0.5.

On the other hand, the rate of the overall intensity of terminal carbonyls to that of bridging ones, at lower temperatures, is smaller ($R_{T/Br}$ = 5.8 and 5.7) than those found in solutions. This surprising fact suggests that practically every molecule contains a bridge or bridges.

The frequencies of both pairs $\nu_{A'}$, $\nu_{B'}$ and $\nu_{C'}$, $\nu_{D'}$ slightly but significantly differ from the respective ones in solutions, indicating that the bridging structure of the molecules bonded to the silica might somehow differ from that found in other systems. The values of angles $\phi$ of both pairs are also smaller than those calculated for the $SiO_2$/Nujol system showing the molecules are more distorted.

It is worth mentioning that the band $\nu_H$ might formally be regarded as the asymmetric combination of the stretching modes of a double bridging system with very long C–O distances, whose symmetric pair would be expected at about 1860 $cm^{-1}$. However, no component at this frequency has been found, which suggests that this component, if it exists, should be of very low or zero intensity, and consequently angle $\phi$ should be 180°. Such a coplanar double bridging structure is hardly probable because there is a general tendency in all double bridging systems identified: lower frequencies (longer C–O bond length) are accompanied with a closing of the angle $\phi$.

*$H_2FeRu_3(CO)_{13}/SiO_2$/wafer/$H_2$*

The results of the experiment performed in hydrogen (see Fig. 4k–m and Table II) are similar to those in vacuum, with the difference that in the presence of hydrogen a lower percentage of the molecules have bridging structures ($R_{T/Br}$ = 8.8 at 303 K). With increasing temperature the bridges A'B' and C'D' are stable, however, the monocarbonylic bridge of type H is less stable than in vacuum.

*$H_2FeRu_3(CO)_{13}$/KBr pellet*

Generally, the standard KBr pellet method to measure the IR spectrum of a solid produces spectra characteristic of crystals. However, in the case of the non-rigid molecule of $H_2FeRu_3(CO)_{13}$ the spectrum in both terminal and bridging carbonyl stretching regions (see Figs. 3b and 4n) is rather close to those recorded in polar solvents, suggesting that the crystal structure is quite damaged and the molecules are distorted under the influence of the strong ionic environment. For that reason, we consider this state as an extreme model of adsorbed molecules. In KBr pellet $H_2FeRu_3(CO)_{13}$ is in the bridged form CD with an angle $\phi$ = 126° similar to that found in the polar solvent (123.5°), while on the oxide surfaces the respective angles are considerably inferior (56–67°), except in the case of the $H_2FeRu_3(CO)_{13}/SiO_2$/Nujol system.

*CO Bridges in Pseudo-gas Phase*

From the spectra recorded in nitrogen and argon matrices we could trace three bridging structures. The first is a double bridging one with frequencies close to those of $\nu_A$ and $\nu_B$ of physisorbed molecules. The second, also a double bridging one, which we found in nitrogen matrices, shows similar frequencies to those of $\nu_C$ and $\nu_D$. The third structure is a monocarbonylic bridge, with a frequency (1817 $cm^{-1}$) of type $\nu_H$, and it must be, like the analogous adsorbed species, very unstable, as we could only detect it in nitrogen matrix deposited at low (309 K) sample evaporation temperature.

## Conclusions

Taking into account the results of the studies of bridging carbonyl structures in solutions [1, 2], one would expect that on the oxide surfaces with a large variety of different sites, a wide distribution of different structures would occur resulting in a rather featureless vibrational band pattern. Instead, we found that the spectrum can be resolved into rather well defined components, which may represent well defined surface species.

(a) The first surface species AB, characterized with the frequencies $\nu_A$ and $\nu_B$ (1882 and 1853 $cm^{-1}$), can be assigned to a double bridging carbonyl structure of

molecules bonded by weak physisorption to the oxide support. This type of molecule exists at the very beginning of the surface–cluster interaction ($Al_2O_3$/Nujol and $SiO_2$/Nujol samples), and may be regarded as unperturbed (on $SiO_2$ $\phi = 137°$) or slightly distorted (on $Al_2O_3$ $\phi = 109°$). C–O bonds in this bridging structure are relatively short.

(b) At the end of the cluster–support interaction at room temperature on the $Al_2O_3$ support there is no cluster [6] and no bridging carbonyl left.

(c) The structure A′B′ may be regarded as a second type of surface species characterized with the frequencies 1887 and 1846 $cm^{-1}$; frequencies lying not too far from those of species AB and suggesting shorter C–O distances. However, there are some characteristics suggesting species A′B′ should differ rather more from AB: (i) The separation of both bands is quite different: 29 $cm^{-1}$ for AB and 41 $cm^{-1}$ for A′B′. (ii) Surface species A′B′ is very stable up to rather high temperatures (>413 K). This fact excludes a weak physisorption-type bonding to the surface. We presume molecules with bridging carbonyl structure of type A′B′ may be linked to the surface by chemical bonds.

(d) The next type of surface double bridging structure CD is characterized by the frequencies $\nu_C$ and $\nu_D$ (1872 and 1838 $cm^{-1}$, $d\nu = 33$ $cm^{-1}$). It is analogous with bridging structures in polar solvents. Like species AB, it is also weakly bonded to the surface (physisorbed), and it represents bridging carbonyls with longer C–O distances, which exist at the starting steps of cluster–support interaction.

(e) Surface double bridging structure C′D′ may be derived from structure CD. Its frequencies $\nu_{C'}$ and $\nu_{D'}$ are 1867 and 1830 $cm^{-1}$ ($d\nu = 37$ $cm^{-1}$). It exists as a somehow less stable species on the $SiO_2$ surface in comparison to structure A′B′: it already starts decomposing at 373 K. Angle $\phi$ for this species lies at about 56–67°. C–O distances should be a little longer than in species CD.

(f) On the $Al_2O_3$ surface an additional double bridging structure EF has been found, resulting in the frequencies $\nu_E = 1896$ and $\nu_F = 1864$ $cm^{-1}$ ($d\nu = 32$ $cm^{-1}$), with a very close angle $\phi$ (68–52°). The frequencies indicate extremely short C–O bonds.

(g) On $Al_2O_3$ a band $\nu_G$ at about 1909 $cm^{-1}$ has been found that is assigned to monocarbonylic, very asymmetric, 'incipient' CO bridges (structure G).

(h) The next bridging structure H, only detected on the $SiO_2$ surface, is supposed a monocarbonylic one, which has a considerably longer C–O distance. Its frequency lies between 1822–1816 $cm^{-1}$.

(i) By thermal treatment of a supported cluster in vacuum the stability of the different bridging structures is as follows: A′B′ > C′D′ > H.

(j) By thermal treatment in hydrogen the temperature range of the stability of bridges is lower than in vacuum by 60–80 K.

(k) Matrix isolation experiments supply evidences of different conformers of the $H_2FeRu_3(CO)_{13}$ molecule.

(l) Two double bridging (type AB and CD) and one monobridging (type H) carbonylic structures have been detected in noble gas matrices. Further analogies have been found between double bridging structures AB and CD and those found in solutions and in KBr pellet. An analogous monobridging structure of surface species type H has also been detected in KBr pellet.

## Acknowledgements

Thanks are due to A. Vizi-Orosz for preparation of $H_2FeRu_3(CO)_{13}$ and to S. Simonetti and G. Radiciotti for technical assistance.

## References

1 S. Dobos, S. Nunziante-Cesaro and M. Maltese, *Inorg. Chim. Acta, 113,* 167 (1986).
2 S. Dobos, S. Nunziante-Cesaro, *J. Mol. Struct., 142,* 579 (1986).
3 V. L. Kuznetsov, A. Bell and Y. I. Yermakov, *J. Catal., 65,* 374 (1980).
4 H. Knözinger, Y. Zhao, B. Teschke, R. Barth, R. Epstein, B. C. Gates and J. P. Scott, *Faraday Discussion, 72,* 53 (1981).
5 (a) A. Zecchina, E. Guglielminotti, A. Bosi and M. Camia, *J. Catal., 74,* 225 (1982); (b) E. Guglielminotti, A. Zecchina, A. Bosi and M. Camia, *J. Catal., 74,* 240 (1982); (c) *74,* 252 (1982).
6 S. Dobos, I. Böszörményi, J. Mink and L. Guczi, *Inorg. Chim. Acta, 120,* 135 (1986).
7 S. Dobos, I. Böszörményi, J. Mink and L. Guczi, *Inorg. Chim. Acta, 120,* 145 (1986).
8 D. B. W. Yawney and F. G. A. Stone, *J. Chem. Soc. A,* 502 (1969).
9 J. J. Turner and M. Poliakoff, *J. Chem. Soc. A,* 654 (1971).
10 B. I. Swanson, L. H. Jones and R. R. Ryan, *J. Mol. Spectrosc., 45,* 354 (1973).
11 G. L. Geoffroy and W. L. Gladfelter, *J. Am. Chem. Soc., 99,* 6775 (1977).
12 L. Milone, S. Aime, E. W. Randall and E. Rosemberg, *J. Chem. Soc., Chem. Commun.,* 452 (1975).
13 S. Dobos, I. Böszörményi, J. Mink and L. Guczi, *Inorg. Chim. Acta, 132* (1987) in press.